

Also if sufficient data were available it would be a simple matter to include rate information by showing free energies of activation as free energy humps<sup>2,3</sup> associated with each couple.

An additional example of a free energy oxidation

(2) Bancroft and Magoffin, *J. Franklin Inst.*, **224**, 283 (1937).

(3) Remick, *THIS JOURNAL*, **69**, 94 (1947).

state diagram calculated, using data from Latimer, is shown in Fig. 4.

The author wishes to acknowledge helpful discussions of this idea with many of his colleagues at Northwestern University.

EVANSTON, ILL.

RECEIVED DECEMBER 2, 1950

[CONTRIBUTION FROM THE DEPARTMENT OF METALLURGY, MASSACHUSETTS INSTITUTE OF TECHNOLOGY]

## The Thermodynamic Properties of Liquid Ternary Cadmium Solutions<sup>1</sup>

BY JOHN F. ELLIOTT AND JOHN CHIPMAN

The ternary systems cadmium-lead-bismuth, cadmium-lead-antimony and cadmium-lead-tin have been investigated by electrode-potential methods over the temperature interval of 380 to 600°. The properties  $\Delta F^\circ$ ,  $\Delta S^\circ$ ,  $\Delta H$ ,  $\Delta F_i^\circ$ ,  $L_i$  and activities are computed for the three ternary solutions and the lead-tin binary solution at 500°. They are best summarized by reference to the appropriate figures in the text.

Up to the present time, thermodynamic studies of liquid alloys containing more than two components have been concentrated on very small portions of the multicomponent field. Consequently highly specific information has been accumulated and little is known regarding the general thermodynamic behavior of multicomponent metallic systems. Recently Darken<sup>2</sup> has clarified the treatment of tertiary systems by showing that a molal thermodynamic property (and in turn the corresponding partial molal quantities) may be computed for the whole of an isobaric, isothermal, single-phase ternary system if the partial molal property of one component is known over the ternary field. Compositions represented by a line with constant ratio of component 1 to component 3 crossing the ternary field to the apex of pure component 2 are treated as a binary system. Darken has demonstrated that the familiar methods

for determining partial molal properties are applicable to this pseudo-binary system.

This paper describes an electrochemical study of three ternary metallic systems in the liquid phase and utilizes Darken's methods to determine the molal and partial molal properties, free energy, heat of solution and entropy. The electrode-potential method described in a previous paper<sup>3</sup> was used to evaluate the thermodynamic properties of cadmium for several pseudo-binary lines crossing each of the ternary fields in the systems cadmium-lead-bismuth, cadmium-lead-antimony and cadmium-lead-tin. The properties of the component binary systems are taken from the earlier paper and from other published data.

### Experimental Method

The experimental technique, equipment and materials will be described only briefly, as they have been discussed in considerable detail in the preceding paper.<sup>3</sup> The electrode-potential measurements were obtained from four-legged Pyrex-glass cells (Fig. 1). The cathode alloys were placed in three of the four legs and the pure anode, the most electropositive metal in the alloys, was placed in the fourth. Liquid electrolyte, the eutectic mixture of lithium and potassium chlorides containing about 5% of the chloride of the most electropositive metal, was poured in the cell. The system was sealed and evacuated to degas the electrodes and electrolyte. Subsequently the lower portion of the cell was placed in a lead-bath and the potentials between the cathodes and anode were obtained for five to six temperatures between 380 and 600°. Measurements above 575° were discarded since unsteady readings were noted occasionally near 600°. The estimated limit of error in the data is approximately 0.05 mv. for potentials below 10 mv. and 0.10 mv. for those above.

### Cadmium-Lead-Bismuth Solution

Two master binary alloys with the atomic ratios of lead to bismuth of 1.974:1.000 and 1.000:2.000 were prepared. (For convenience these alloys will subsequently be called Series 1 and 2, respectively, and the atomic ratios of lead to bismuth will be approximated by the figures 2:1 and 1:2.) Pure bismuth and lead were alloyed at 350° under an eutectic cover of potassium and lithium chlorides and then sticks of the alloys were chill cast. Subsequent analyses of the alloys and of electrodes prepared from the alloys showed that there was no significant segregation during casting.

The cell electrodes were prepared by alloying in the cell legs previously weighed sticks of cadmium and master alloys. Preparing the electrodes in this manner gave two series of alloys which cross the ternary field from the base binary

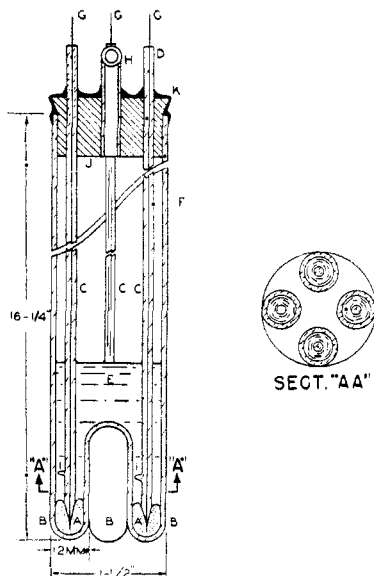


Fig. 1.—Design of cell.

(1) This paper is based upon a thesis submitted by John F. Elliott in partial fulfillment of the requirements for the degree of Doctor of Science at the Massachusetts Institute of Technology.

(2) I. S. Darken, *THIS JOURNAL*, **78**, 2009 (1950).

(3) J. F. Elliott and J. Chipman, *Trans. Faraday Soc.*, **47**, 138 (1951).

system, lead-bismuth, to the cadmium apex along the lines of constant atomic ratios of lead to bismuth of 2:1 and 1:2. Chemical analyses of approximately 30% of the electrodes taken from the cells after completion of the runs indicated that the alloy compositions as weighed were correct. Compositions of the electrodes are shown in Table I.

TABLE I

CELL COMPOSITIONS AND POTENTIALS AT 500° FOR THE CADMIUM-LEAD-BISMUTH SOLUTION

Cell no.	$N_{Cd}$	$E(\text{mv.})$	$\frac{\partial E}{\partial T} \times 10^3$ mv./°C.
Cadmium-Alloy 1 Series $N_{Pb}:N_{Bi} = 1.974$			
85-4	0.9376	1.79	3.51
83-3	.8775	3.40	6.89
83-4	.8119	5.09	12.3
72-5	.6914	7.88	21.9
74-2	.6723	8.43	22.4
71-2	.6555	9.13	23.4
71-4	.5699	11.01	29.1
74-4	.5631	11.73	32.2
79-4	.4199	17.29	46.6
71-5	.3143	23.77	60.2
74-5	.2462	29.64	72.7
77-5	.1995	34.33	78.0
81-5	.1125	50.07	106.1
78-5	.1095	50.79	105.2
Cadmium-Alloy 2 Series $N_{Pb}:N_{Bi} = 0.500$			
84-2	0.9503	1.50	2.45
84-3	.8624	4.08	8.26
84-4	.8221	5.13	11.2
77-2	.7793	4.46	11.5
81-2	.6291	12.47	30.4
81-3	.5523	15.97	37.7
77-3	.4291	22.41	44.9
81-4	.2333	39.72	76.9
77-4	.1182	59.62	101.0
Lead-Bismuth Series			
80-2	0.9011	3.57	4.34
80-3	.5791	22.71	22.3
82-2	.5017	29.60	31.2
80-4	.3333	47.23	47.4
82-4	.1357	86.08	89.4

The potential of each electrode relative to pure cadmium was plotted as a linear function of temperature and carefully interpolated for the 500° point which is shown in Table I. The temperature coefficient is also recorded.

The potential of lead against five binary lead-bismuth electrodes was determined using as electrolyte lead chloride in fused KCl-LiCl solution. The results are recorded in Table I and are compared with those of earlier investigators<sup>4a,b</sup> in Fig. 4.

### Calculations

The partial molal free energy, entropy and heat of solution of cadmium in the alloys (the standard state in all cases is the pure metal) are obtained directly from the data by means of the equations

$$\Delta \bar{F}_{Cd} = -(2\mathcal{F}E)_{T,P} \quad (1)$$

$$\Delta \bar{S}_{Cd} = 2\mathcal{F}(\partial E/\partial T)_{N,P} \quad (2)$$

$$\Delta \bar{H}_{Cd} = \bar{L}_{Cd} = -2\mathcal{F}[E - T(\partial E/\partial T)_{N,P}] \quad (3)$$

Here  $E$  is the cell potential and  $\mathcal{F}$  is the Faraday equivalent.

It is convenient to employ "excess" molal and partial molal properties defined as the observed value minus that for an ideal solution of the same mole fraction. The superscript  $x$  is used to denote

such quantities, which are formally defined by the equations<sup>4</sup>

$$\Delta \bar{F}_i^x = \Delta \bar{F}_i - RT \ln N_i = RT \ln a_i/N_i \quad (4)$$

$$\Delta \bar{S}_i^x = \Delta \bar{S}_i + R \ln N_i = (\bar{L}_i - \Delta \bar{F}_i^x)/T \quad (5)$$

$$\bar{L}_i^x = \bar{L}_i = \Delta \bar{H}_i \quad (6)$$

$$\Delta \bar{F}^x = \sum_1^i N_i \Delta \bar{F}_i^x \quad (7)$$

$$\Delta \bar{S}^x = \sum_1^i N_i \Delta \bar{S}_i^x = (\Delta \bar{H} - \Delta \bar{F}^x)/T \quad (8)$$

$$\Delta \bar{H}^x = \Delta \bar{H} = \sum_1^i N_i \bar{L}_i \quad (9)$$

For purposes of graphical calculation it is convenient to plot such functions as  $\Delta \bar{F}_i^x/(1 - N_i)^2$  and  $\bar{L}_i/(1 - N_i)^2$ . The experimental data are plotted in this manner in Figs. 2 and 3 which show these two functions for cadmium in each of the four (pseudo) binary solutions

(A) Cd-Pb, (B) Cd-Pb:Bi = 2:1, (C) Cd-Pb:Bi = 1:2, (D) Cd-Bi.

This method of plotting is especially useful since it provides both a sensitive means for comparison of data and an accurate graphical integration of the Gibbs-Duhem equation. In ternary solutions it has a special usefulness in the treatment recently developed by Darken<sup>2</sup> which is summarized in the following paragraphs.

The slope-intercept method for computing partial molal quantities is based on the equation, in which  $G$  represents any extensive property

$$\bar{G}_2 = G + (1 - N_2)[\partial G/\partial N_2]_{N_1/N_3} \quad (10)$$

Dividing through by  $(1 - N_2)^2$  and rearranging terms

$$\left[ \frac{\partial G/(1 - N_2)}{N_2} \right]_{N_1/N_3} = \bar{G}_2/(1 - N_2)^2 \quad (11)$$

There are two alternate procedures for integrating Equation (11) along the line of constant  $N_1/N_3$ , the first of which is to integrate along the line of constant  $N_1/N_3$  from  $N_2$  equals zero at the base line to  $N_2$ . The resulting equation for calculating the excess molal property of the solution is

$$G^x = (1 - N_2) \left[ \int_0^{N_2} \frac{\bar{G}_2^x}{(1 - N_2)^2} dN_2 + G_{\text{binary } 1-3}^x \right]_{N_1/N_3} \quad (12)$$

This is identical with the expression for a true binary solution with the addition of the integration constant  $G_{\text{binary } 1-3}^x$  which represents the value of  $G^x$  at the base-line binary 1-3 (where  $N_2 = 0$ ), and with the added restriction that the integration is to be taken along a line of constant ratio  $N_1/N_3$ .

The second method is to integrate Equation (11) from  $N_2$  equals one to  $N_2$ . The resulting equation for computing the molal property of the solution in this case is

$$G^x = (1 - N_2) \left[ \int_1^{N_2} \frac{\bar{G}_2^x}{(1 - N_2)^2} dN_2 \right]_{N_1/N_3} + N_1[\bar{G}_1^x]_{N_2=1} + N_3[\bar{G}_3^x]_{N_2=1} \quad (13)$$

In the last two terms the bracketed quantities refer to the infinitely dilute binary solutions of

(4) (a) H. S. Strickler and H. Seltz, THIS JOURNAL, 58, 2085 (1936); (b) C. Wagner and G. Engelhardt, Z. Physik. Chem., A100, 241 (1932).

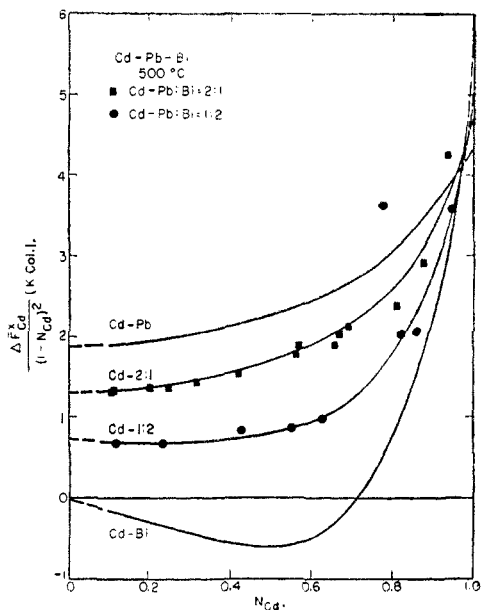


Fig. 2.—Free energy function of cadmium at 500° in the cadmium-lead-bismuth solution.

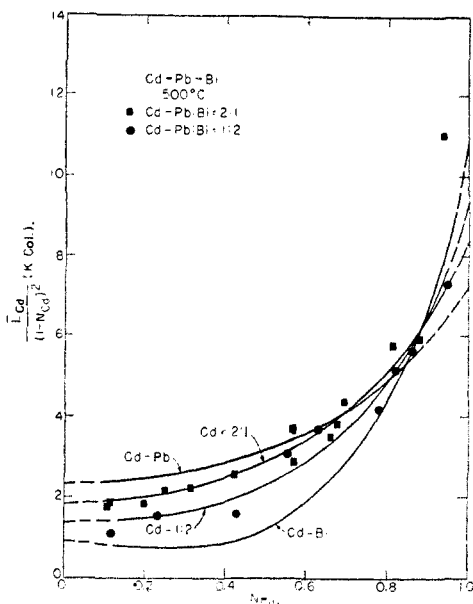


Fig. 3.—Heat of solution function of cadmium at 500° in the cadmium-lead-bismuth solution.

components 1 and 3, respectively, in component 2. The values of  $[\bar{G}_1^x]_{N_2=1}$  and  $[\bar{G}_3^x]_{N_2=1}$  are found from the respective binaries as the integral

$$\int_0^1 \bar{G}_2^x / (1 - N_2)^2 dN_2$$

When  $\bar{G}_2^x$  is known for all compositions of the ternary system,  $G^x$  may be evaluated at all compositions by Equation (13), or alternatively by Equation (12) if this property is known for the binary system 1-3. The data of Table I, together with the previously published data on the binary systems, provide values of  $\Delta F_{Cd}^x$  and  $L_{Cd}^x$  in the ternary system and corresponding values for lead in the base binary which are sufficient to inter-

polate the molal values  $\Delta F^x$  and  $\Delta H$  over the entire system.

The properties of lead in the lead-bismuth binary are plotted in Fig. 4. The system is "regular" within the limits of our experimental error so that  $\Delta S^x = 0$  and  $\Delta F^x$  and  $\Delta H$  are equal. Values of these functions for the 2:1 and 1:2 compositions are recorded in Table II as "observed."

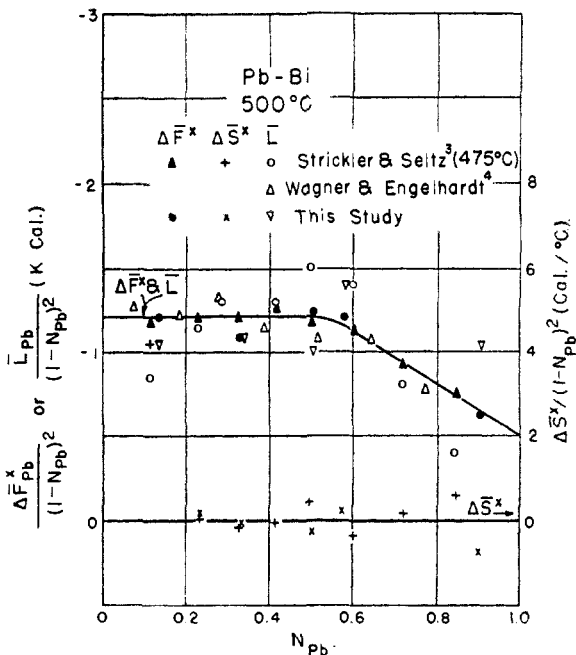


Fig. 4.—Thermodynamic functions of lead in the lead-bismuth solution.

As a test of the consistency of the data the same functions for the binary system are calculated from the ternary data. Comparison of Equations (12) and (13) yields

$$G_{\text{binary 1-3}}^x = - \left[ \int_0^1 \frac{\bar{G}_2^x}{(1 - N_2)^2} dN_2 \right]_{N_1/N_3} + N_1 [\bar{G}_1^x]_{N_2=1} + N_3 [\bar{G}_3^x]_{N_2=1} \quad (14)$$

Values of  $\Delta F^x$  and  $\Delta H$  calculated from Equation (14) along each of the pseudo-binary lines are recorded in Table II as "Predicted." The agreement is excellent.

TABLE II

PROPERTIES OF THE LEAD-BISMUTH SOLUTIONS AT 500°

	$N_{Pb}:N_{Bi} = 2:1$		$N_{Pb}:N_{Bi} = 1:2$	
	Obsd. <sup>a</sup>	Predicted <sup>b</sup>	Obsd. <sup>a</sup>	Predicted <sup>b</sup>
$\Delta F^x$ , cal.	-265	-250	-270	-280
$\Delta H$ , cal.	-265	-250	-270	-250

<sup>a</sup> Obtained from binary Pb-Bi data (Fig. 4). <sup>b</sup> Obtained from ternary Cd-Pb-Bi data (Figs. 2 and 3).

The  $\Delta F^x$  and  $\Delta H$  curves for the 2:1 and 1:2 lines crossing the ternary field are computed by Equation (12). The integral on the right is the area from 0 to  $N_2$  under the appropriate curve in Fig. 2 or 3 and the integration constant is obtained from the "observed" column in Table II. The molal curves for the cadmium-lead and cadmium-bismuth binary solutions were reported in the

previous paper.<sup>3</sup> From the  $\Delta F^x$  and  $\Delta H$  curves for three binary and two pseudo-binary lines are interpolated the ternary molal surfaces shown in Figs. 5 and 6. The ternary  $\Delta S^x$  surface shown in Fig. 7 is obtained from Figs. 5 and 6 by Equation (8).

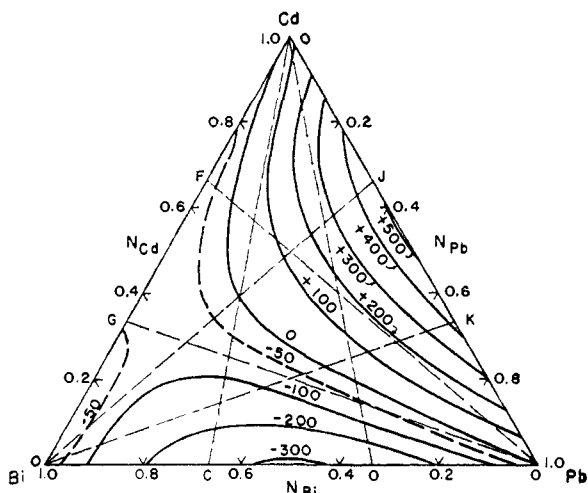


Fig. 5.—Excess molal free energy of solution surface ( $\Delta F^x$ ) for the cadmium-lead-bismuth solution at 500° in 100 calorie steps.

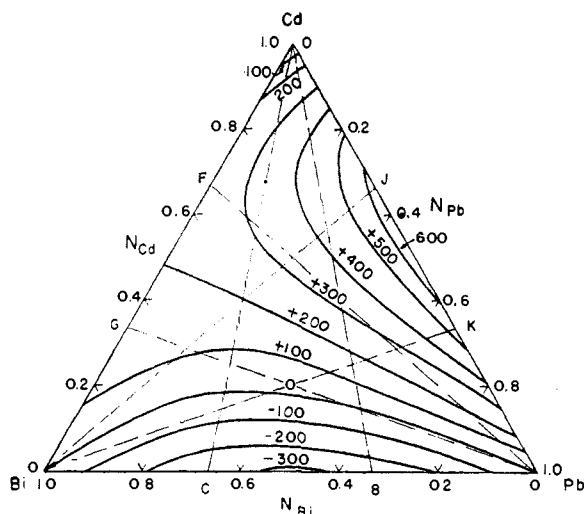


Fig. 6.—Molal heat of solution surface ( $\Delta H$ ) for the cadmium-lead-bismuth solution at 500° in 100 calorie steps.

**Partial Molal Quantities.**—The  $\Delta F_i^x$  and  $L_i$  curves for each of the three components for the binary and pseudo-binary lines of the ternary system are shown in Figs. 8 and 9. Those for the boundary cadmium-lead and cadmium-bismuth binaries (A, D, E and I) were reported in the previous paper.<sup>3</sup> The curves for cadmium in the pseudo-binary lines and for lead in the lead-bismuth solution (B, C and H) are obtained directly from the  $\bar{G}_2^x/(1 - N_2)^2$  curves in Figs. 2, 3 and 4 by multiplying each point on the curves by  $(1 - N_2)^2$ .  $\Delta \bar{F}_{Bi}^x$  and  $\bar{L}_{Bi}$  curves (L) for the lead-bismuth solution are computed from Fig. 4 by the following form of the Gibbs-Duhem equation

$$\bar{G}_{Bi}^x = -\frac{\bar{G}_{Pb}^x}{(1 - N_{Pb})^2} N_{Pb} N_{Bi} + \int_0^{N_{Pb}} \frac{\bar{G}_{Pb}^x}{(1 - N_{Pb})^2} dN_{Pb} \quad (15)$$

Curves F, G, J and K are obtained by the slope-intercept method (Equation 10). The profiles of the  $\Delta F^x$  and  $\Delta H$  surfaces for the four pseudo-binary lines crossing from lead to F and G and from bismuth to J and K are constructed. The intercept of the slope of the profile at a given composition with the lead or bismuth axis yields  $\Delta \bar{F}_i^x$  or  $\bar{L}_i$  for that composition. The scale on the right of Fig. 8 gives the logarithm of the activity coefficient.

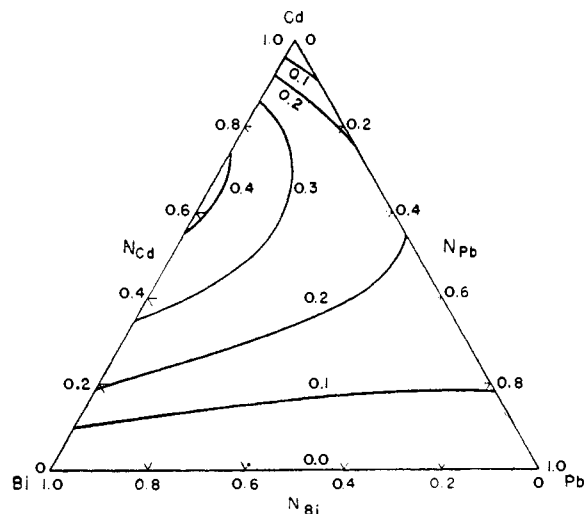


Fig. 7.—Excess molal entropy of solution surface ( $\Delta S^x$ ) for the cadmium-lead-bismuth solution at 500° in 0.1 calories/°C. steps.

Activity surfaces for the three components of the solution are depicted by the isoactivity lines in Fig. 10. The activities are computed from the  $\Delta \bar{F}_i^x$  curves in Fig. 8 by Equation 4. The isoactivity lines are interpolated from the resulting activity curves.

#### Cadmium-Lead-Antimony Solution

Two master alloys of lead and antimony with atomic ratios of 2:1 and 1:2 (Series 3 and 4, respectively), were prepared in the same manner as were the alloy Series 1 and 2. Electrodes were formed by alloying these alloys with cadmium in the cell legs as before, but chemical analyses were required of all of the ternary alloys after their removal from the cell legs. This was because the master alloys were segregated and because apparently some volatilization of antimony, probably as a chloride, occurred during the evacuation step prior to the operation of the cell. The electrode analyses and electrode-potential measurements at 500° (obtained from data over the interval from 390 to 575°) for these two alloy series are shown in Table III.

The potential of lead against three lead-antimony electrodes was determined as described for the lead-bismuth series. The results are recorded in Table III.

Segregation in the lead-antimony master alloys caused the cathode compositions to fall on both sides of the lines of ratios of lead to antimony of 2:1 and 1:2 crossing the ternary field. As a result the observed data could not be used directly in the calculations so they were corrected to bring each point on a line of a constant ratio of lead to antimony, i.e., 2:1 and 1:2.

The corrective procedure was as follows. The functions  $\Delta \bar{F}_{Ca}^x/(1 - N_{Ca})^2$  and  $\Delta \bar{S}_{Ca}^x/(1 - N_{Ca})^2$  were computed for each point at 500°. The computed points were plotted

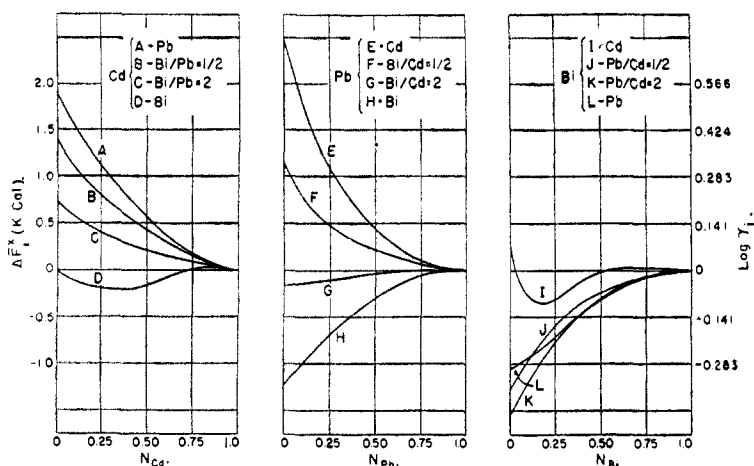


Fig. 8.—Excess partial molal free energy of solution curves in the cadmium-lead-bismuth solution at 500°.

versus the atom fraction of cadmium in four lines corresponding to those shown in Fig. 11, and smooth curves were drawn through them. Points at the same cadmium concentration as of the datum being corrected were taken from these curves and the four points were plotted as a profile of the function for the constant cadmium line crossing the ternary field. From this profile the corrected value which is listed in Table III was read at the 2:1 or 1:2 ratio of lead to antimony. The corrected values of the heat of solution function were calculated from the free energy and entropy values by Equation (5).

### Calculations

The free energy and heat of solution functions of cadmium in the two boundary binary solutions<sup>3</sup> and the two lines of lead:antimony of 2:1 and 1:2 for the ternary system are plotted in Figs. 11 and 12. The experimental points are the corrected values from Table III. Curves of these same functions for lead in the third boundary binary solution, lead-antimony, are plotted in Fig. 13.

TABLE III  
CELL COMPOSITIONS AND POTENTIALS AT 500° FOR THE CADMIUM-LEAD-ANTIMONY SOLUTION

Cell No.	$N_{Cd}$	$N_{Pb}/N_{Sb}$	$E$ (mv.)	$\frac{\partial E}{\partial T} \times 10^3$ (mv./°C.)	$\Delta \bar{F}_{Cd}^E / (1 - N_{Cd})^{\dagger}$		$\Delta \bar{S}_{Cd}^E / (1 - N_{Cd})^{\dagger}$		$L_{Cd} / (1 - N_{Cd})^{\dagger}$
					Obsd.	Cal. Corrected <sup>a</sup>	Obsd. Cal./°C.	Corrected <sup>a</sup>	
Cadmium-Alloy 3 Series $N_{Pb}:N_{Sb} = 2.00$									
86-2	0.9498	1.789	1.52	2.70	3880	3930	8.8	8.7	10600
86-3	.8958	1.824	3.08	5.88	2470	2530	4.7	4.6	6080
102-2	.8848	1.961	3.36	6.58	2490	2500	4.5	4.5	6970
102-4	.8002	1.842	6.02	13.2	1620	1690	4.2	4.1	4850
86-4	.7969	1.741	6.08	13.3	1660	1770	3.9	3.8	4710
87-2	.6758	2.188	9.69	22.0	1490	1410	2.3	2.3	3190
87-3	.5928	1.900	13.28	29.3	1150	1190	1.9	1.9	2660
87-4	.4926	1.846	18.98	39.6	825	910	1.6	1.6	2150
88-2	.3864	2.160	25.73	51.3	729	647	1.3	1.3	1650
98-4	.3731	2.548	25.23	51.7	892	629	1.1	1.1	1480
88-3	.2497	1.932	40.99	67.7	428	460	0.64	0.64	954
88-4	.0772	1.896	70.50	98.5	804	850	-0.63	-0.62	370
Cadmium-Alloy 4 Series $N_{Pb}:N_{Sb} = 0.500$									
89-2	0.9581	0.258	1.63	2.62	-5300	-5300	20	19	9400
89-3	.8973	.5059	3.28	6.11	1430	1430	6.3	6.3	6300
89-4	.8096	.5075	6.74	13.5	360	345	5.5	5.5	4600
90-2	.6985	.5029	12.36	23.1	-210	-216	3.8	3.8	2720
90-3	.5910	.4932	20.18	32.0	-732	-710	2.6	2.6	1300
90-4	.4984	.5009	28.51	40.3	-976	-978	1.9	1.9	490
97-2	.3980	.4894	40.27	45.4	-1220	-1190	0.72	0.71	-642
97-3	.2326	.4936	63.47	65.4	-1167	-1150	0.20	0.20	-995
97-4	.0963	.4480	94.54	103.6	-940	-824	0.16	0.16	-700
Lead-Antimony Series									
104-2	0.8952	8.542	3.69	5.1					
104-3	.7668	3.288	9.08	12.8					
104-4	.6902	2.228	12.90	17.3					

<sup>a</sup> Corrected to 2:1 or 1:2 ratio of Pb:Sb with  $N_{Cd}$  unchanged.

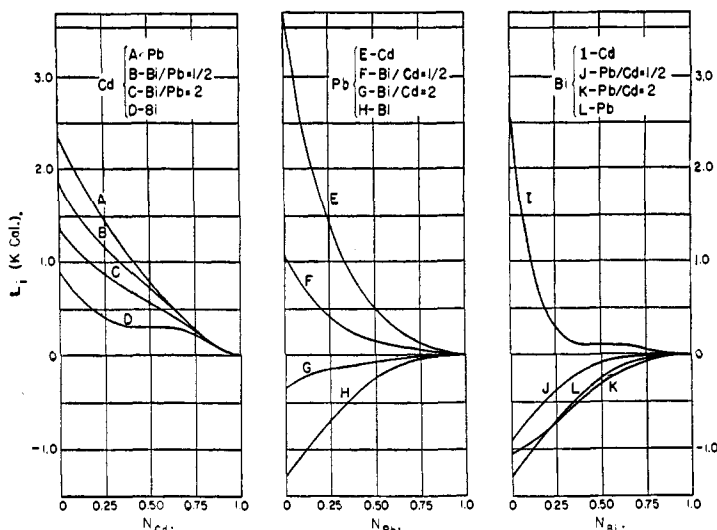


Fig. 9.—Relative partial molal heat of solution curves in the cadmium-lead-bismuth solution at 500°.

The points are obtained from Seltz and De Witt's<sup>5</sup> data and from Table III. Since the melting point of antimony is above 500°, the points shown above about 65% antimony were obtained by downward extrapolation of Seltz and De Witt's data for higher temperatures.

cadmium-lead-bismuth solution. Table IV contains the integration constants for Equation (12).

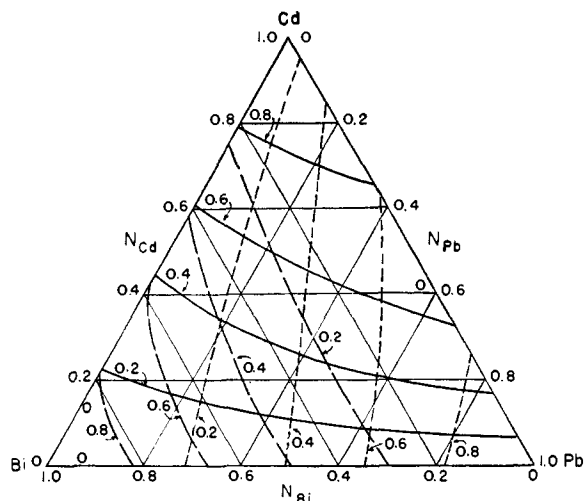


Fig. 10.—Isoactivity lines in the cadmium-lead-bismuth solution at 500°: activity lines: —, cadmium; - - -, lead; - · - ·, bismuth.

**Excess Molal and Partial Molal Quantities.**— Calculation of the  $\Delta F^x$  and  $\Delta H$  surfaces for this solution from Figs. 11, 12 and 13 is carried out in the same way as previously described for the

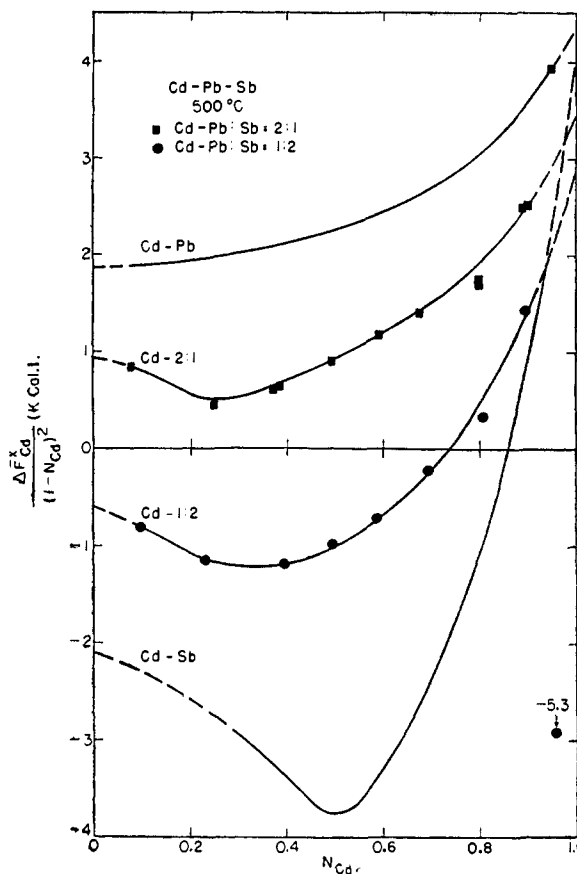


Fig. 11.—Free energy function of cadmium at 500° in the cadmium-lead-antimony solution.

TABLE IV  
PROPERTIES OF THE LEAD-ANTIMONY SOLUTIONS AT 500°

	$N_{Pb}:N_{Sb} = 2:1$		$N_{Pb}:N_{Sb} = 1:2$	
	Obsd. <sup>a</sup>	Predicted <sup>b</sup>	Obsd. <sup>a</sup>	Predicted <sup>b</sup>
$\Delta F^x$ , cal.	-98	-225	-103	-183
$\Delta H$ , cal.	-36	-40	-80	+338

<sup>a</sup> Obtained from Pb-Sb binary data (Fig. 13). <sup>b</sup> Obtained from Cd-Pb-Sb ternary data (Figs. 11 and 12).

(5) H. Seltz and B. J. De Witt, THIS JOURNAL, 61, 2594 (1939).

Again the observed values of  $G_{binary 1-3}^x$  are used in calculating the excess molal surfaces in Figs. 14, 15 and 16 as there is less uncertainty in them than for the predicted values.

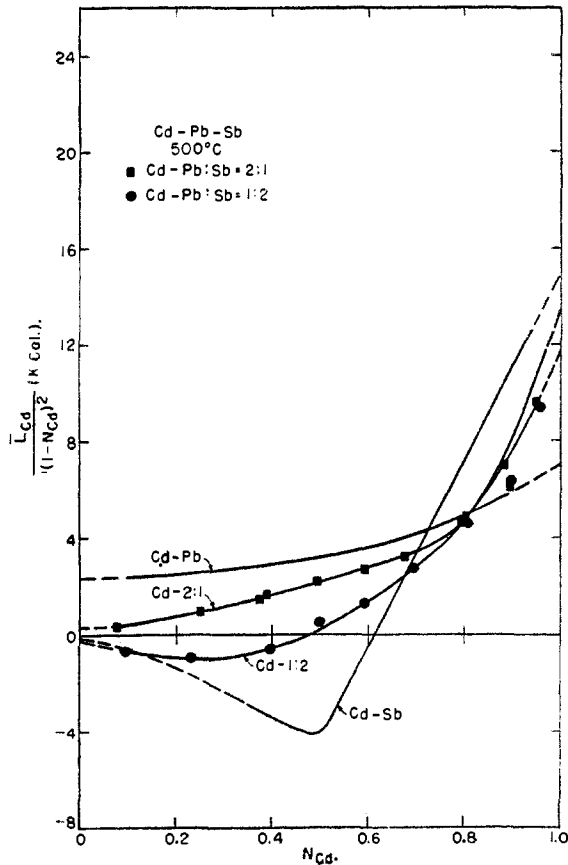


Fig. 12.—Heat of solution function of cadmium at 500° in the cadmium-lead-antimony solution.

The curves of  $\Delta\bar{F}^x$ ,  $\bar{L}_i$  and the isoactivity lines in Figs. 17, 18 and 19 are obtained from the ternary  $\Delta F^x$  and  $\Delta H$  surfaces (Figs. 14 and 15) and from the free energy and heat of solution functions in Figs. 11, 12 and 13. The computational procedure is the same as described for the cadmium-lead-bismuth system.

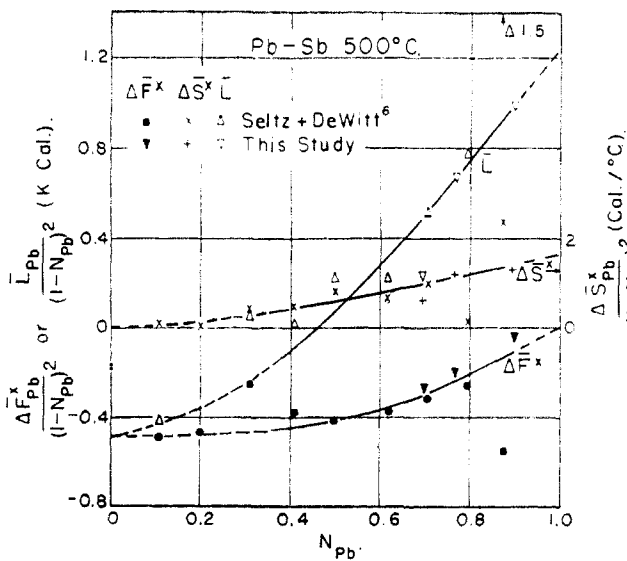


Fig. 13.—Thermodynamic functions of lead in the lead-antimony solution.

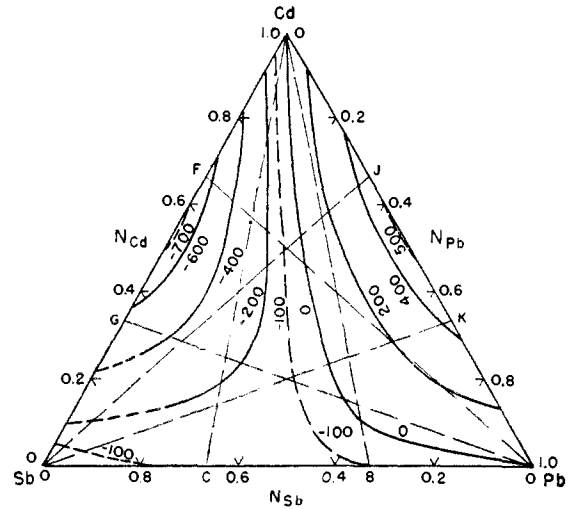


Fig. 14.—Excess molal free energy of solution surface ( $\Delta F^x$ ) for the cadmium-lead-antimony solution at 500° in 200 calorie steps.

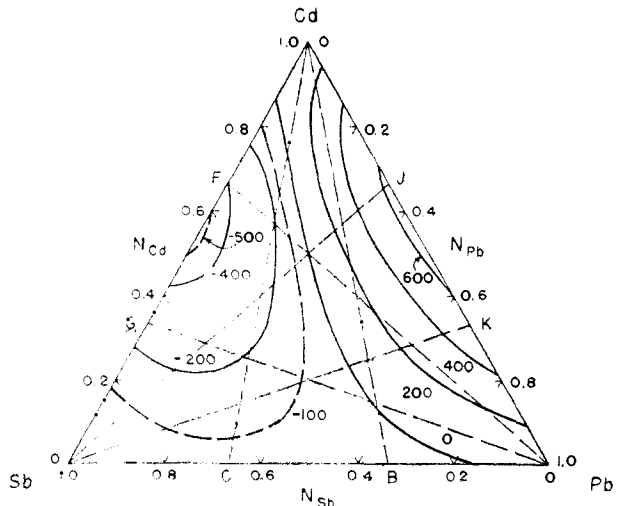


Fig. 15.—Molal heat of solution surface ( $\Delta H$ ) for the cadmium-lead-antimony solution at 500° in 200 calorie steps.

**Cadmium-Lead-Tin Solution**

The cathode alloys were prepared in the same way as described for the preceding two solutions. Chemical analyses of all alloys subsequent to the runs showed that only five of the 21 prepared deviated from the original weighed analyses. The change was a slight loss of tin, probably as a chloride during the evacuation step of the cell preparation. Apparently there was no significant metal transfer because after the runs the anodes and electrolyte contained less than 0.01% tin. The 500° potential and temperature coefficient for each cathode (Table V) were obtained from a plot of the cell potentials *versus* temperature for the interval of 380 to 350°.

**Calculations**

From the data in Table V are computed by Equations (1), (3), (4) and (6) the functions  $\Delta\bar{F}_{Cd}/(1-N_{Cd})^2$  and  $\bar{L}_{Cd}/(1-N_{Cd})^2$  which are plotted in Figs. 20 and 21. The two series of points are on the two lines of atomic ratios of lead to tin of 2:1 and 1:2. The deviations of the five alloys mentioned above are insignificant since the

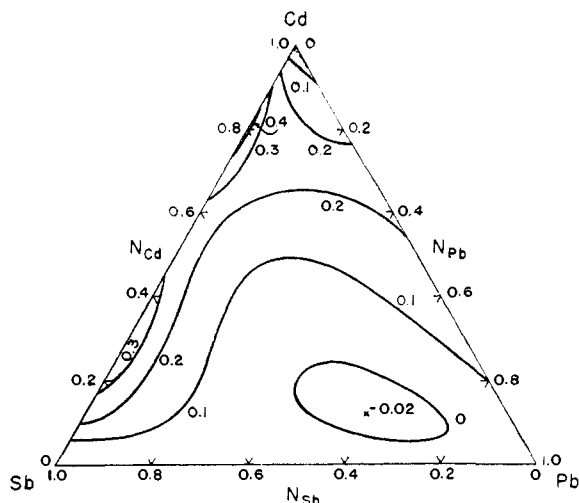


Fig. 16.—Excess molal entropy of solution surface ( $\Delta S^2$ ) for the cadmium-lead-antimony solution at  $500^\circ$  in 0.1 calorie/ $^\circ\text{C}$ . steps.

functions plotted do not change appreciably along lines of constant atomic fractions of cadmium.

**Excess Molal and Partial Molal Surfaces.**—

No data are available for the molal free energy of the lead-tin binary solutions. The electrode potentials of the two metals are too close together for satisfactory measurements, and our attempts to obtain data of the type reported for the lead-bismuth and lead-antimony systems met with failure. Schaefer and Hovorka<sup>6</sup> made measurements in the range of mole fraction of tin from 0.9 to 1 and reported a slight negative deviation from ideality. Körber and Oelsen<sup>7</sup> studied the

TABLE V  
CELL COMPOSITIONS AND POTENTIALS AT  $500^\circ$  FOR THE CADMIUM-LEAD-TIN SOLUTION

Cell No.	$N_{\text{Cd}}$	$N_{\text{Pb}}/N_{\text{Sn}}$	$E$ (mv.)	$\frac{\partial E}{\partial T} \times 10^3$ mv./ $^\circ\text{C}$ .	Composition det. by
Cadmium-Alloy 5 Series $N_{\text{Pb}}:N_{\text{Sn}} = 2.000$					
105-2	0.9546	2.00	1.46	2.43	Weight
105-3	.8930	2.14	3.29	6.27	Analysis
105-4	.7967	2.000	5.71	12.3	Weight
106-2	.6986	2.000	8.40	19.2	Weight
106-4	.6078	2.000	11.06	26.8	Weight
111-2	.5160	2.000	14.33	35.2	Weight
110-2	.4890	2.000	15.51	38.6	Weight
110-3	.4041	2.000	19.50	48.4	Weight
116-2	.4012	1.994	19.30	48.4	Analysis
110-4	.2491	2.000	30.89	73.5	Weight
111-3	.1067	2.000	53.38	118.2	Weight
Cadmium-Alloy 6 Series $N_{\text{Pb}}:N_{\text{Sn}} = 0.500$					
108-2	0.9403	0.527	1.86	2.90	Analysis
108-3	.9055	.500	2.98	5.12	Weight
108-4	.8042	.500	6.08	12.1	Weight
109-2	.6928	.5000	9.63	21.0	Weight
109-4	.5966	.5000	13.09	28.8	Weight
114-3	.5602	.5000	14.72	35.9	Weight
117-2	.4983	.4981	17.03	38.2	Analysis
117-3	.4023	.5000	22.22	48.6	Weight
117-4	.2738	.5079	31.82	68.0	Analysis
111-4	.0992	.5000	60.30	113.8	Weight

heats of solution in the lead-tin binary have been determined by Kawakami<sup>8</sup> whose data are shown in Fig. 22. Similar measurements by Magnus and Manheimer<sup>9</sup> and Von Sampson-Himmelstjerna<sup>10</sup> are less complete and apparently less reliable.

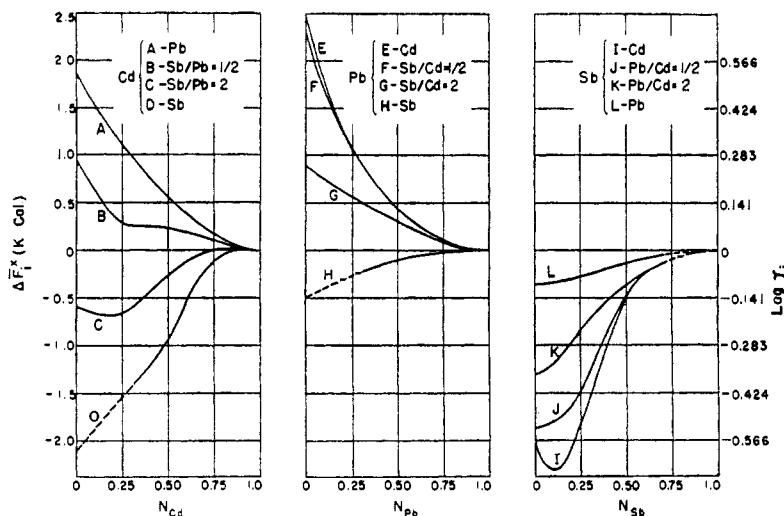


Fig. 17.—Excess partial molal free energy of solution curves in the cadmium-lead-antimony solution at  $500^\circ$ .

equilibrium  $\text{Pb} + \text{SnCl}_2 = \text{Sn} + \text{PbCl}_2$  at  $600^\circ$  using the fused salt pair. Their data do not determine the free energy of the metallic solution since that of the salt solution is unknown. The molal

(6) R. A. Schaefer and F. Hovorka, *Trans. Electrochem. Soc.*, **87**, 479 (1945).

(7) F. Körber and W. Oelsen, *Mitt. Kais. Wilh. Inst. Eisen., Dusseldorf*, **14**, 119 (1932).

Table VI contains the values of the integration constants  $G_{\text{binary } 1-3}^x$  predicted by Equation (14) from the ternary data in Figs. 20 and 21. Also

(8) M. Kawakami, *Science Reports of the Tohoku Imperial University, Japan, Series 1*, **18**, 19 (1929).

(9) A. Magnus and M. Manheimer, *Z. phys. Chem.*, **121**, 267 (1926).

(10) H. O. Von Sampson-Himmelstjerna, *Z. Metallkunde*, **28**, 197 (1936).



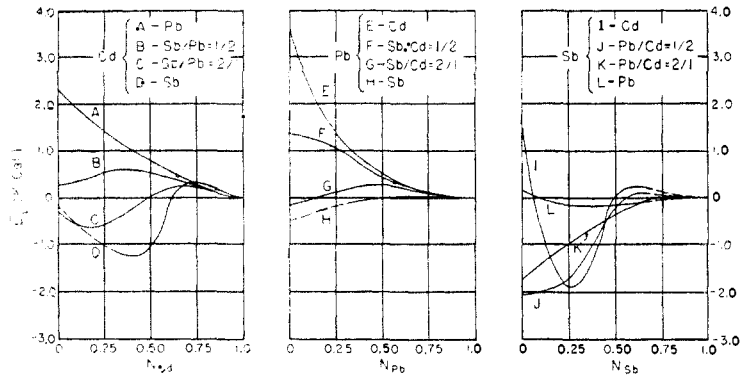


Fig. 18.—Relative partial molal heat of solution curves in the cadmium-lead-antimony solution at 500°.

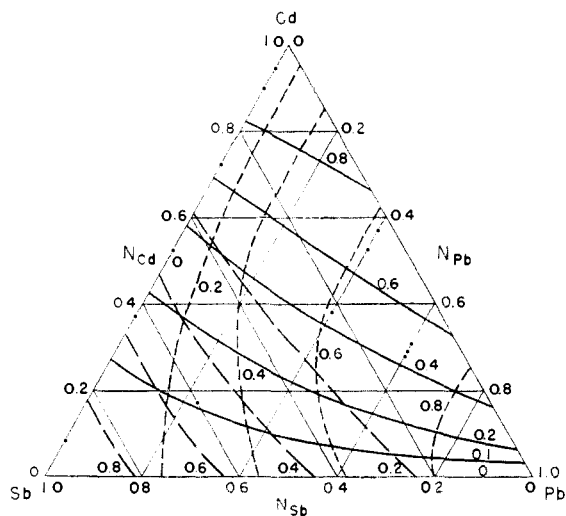


Fig. 19.—Isoactivity lines in the cadmium-lead-antimony solution at 500°: activity lines: —, cadmium; - - - - -, lead; ·····, antimony.

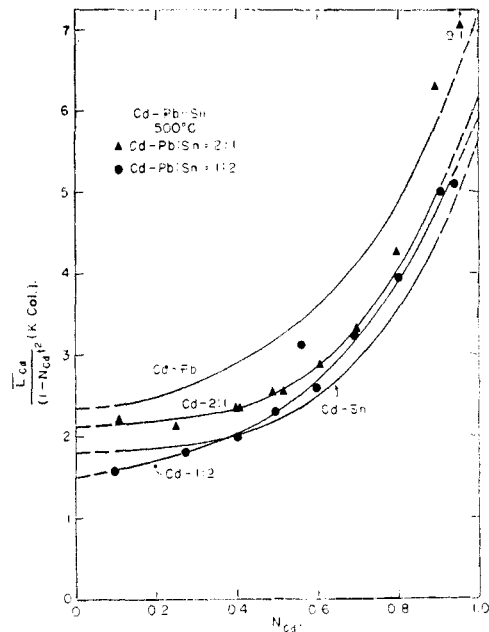


Fig. 21.—Heat of solution function of cadmium at 500° in cadmium-lead-tin solution.

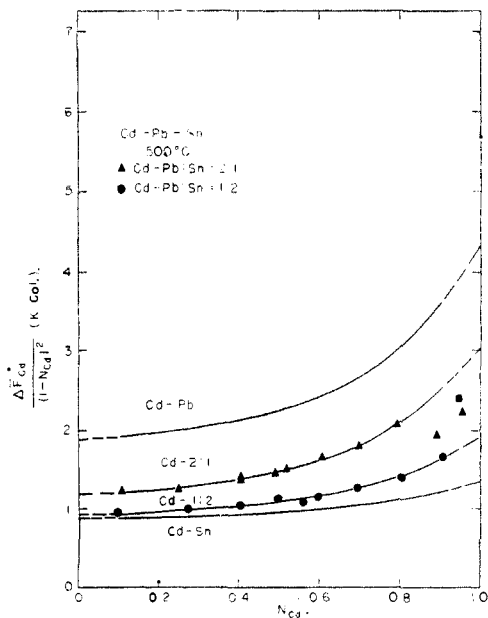


Fig. 20.—Free energy function of cadmium at 500° in the cadmium-lead-tin solution.

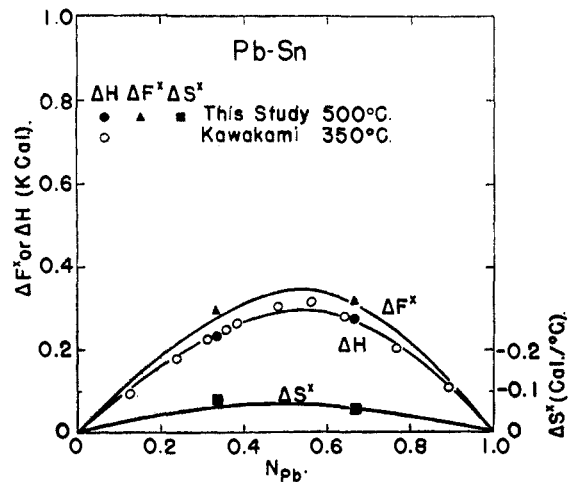


Fig. 22.—Thermodynamic functions in the lead-tin solution.

included are points taken from Kawakami's data for  $\Delta H$  (Fig. 22). There is close agreement

between the predicted and observed values of  $\Delta H$  in Table VI although the calorimetric measurements were made at 350°. The ternary excess

the same as described for the cadmium-lead-bismuth system. The activity curves for the lead-tin system in Fig. 29 are computed from the curves in Fig. 26.

TABLE VI

PROPERTIES OF THE LEAD-TIN SOLUTIONS AT 500°

	$N_{Pb}:N_{Sn} = 2:1$		$N_{Pb}:N_{Sn} = 1:2$	
	Obsd. <sup>a</sup>	Predicted <sup>b</sup>	Obsd. <sup>a</sup>	Predicted <sup>b</sup>
$\Delta F^x$ , cal.	...	320	...	300
$\Delta H$ , cal.	270	280	240	235
$\Delta S^x$ , cal./°C.	...	-0.05	...	-0.08

<sup>a</sup> From Kawakami<sup>8</sup> at 350°. <sup>b</sup> Obtained from ternary Cd-Pb-Sn data (Figs. 20 and 21).

molal surfaces computed by Equation (13) are shown in Figs. 23, 24 and 25.

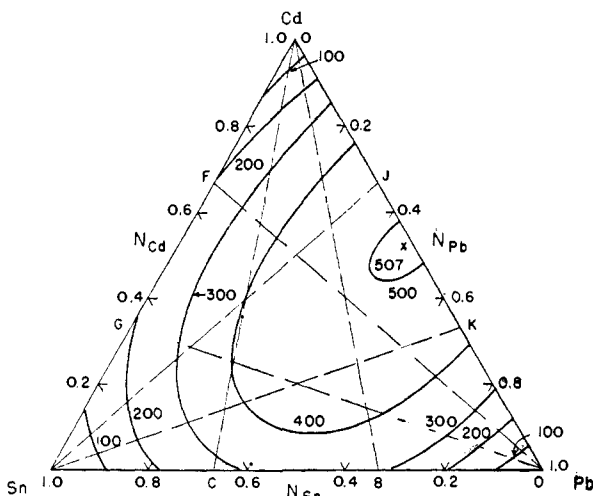


Fig. 23.—Excess molal free energy of solution ( $\Delta F^x$ ) for the cadmium-lead-tin solution at 500° in 100 calorie steps.

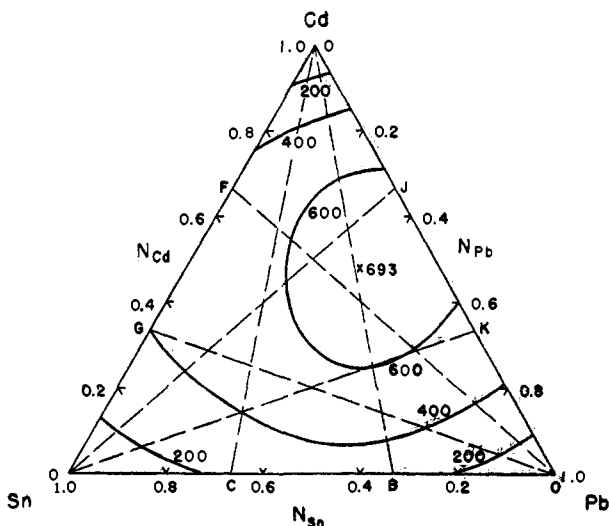


Fig. 24.—Molal heat of solution surface ( $\Delta H$ ) for the cadmium-lead-tin solution at 500° in 200 calorie steps.

The curves of  $\Delta F_i^x$ ,  $\bar{L}_i$  and isoactivity lines in Figs. 26, 27 and 28 are obtained from the ternary  $\Delta F^x$  and  $\Delta H$  surfaces (Figs. 23 and 24) and from the free energy and heat of solution functions in Figs. 20, 21 and 22, the computational procedure being

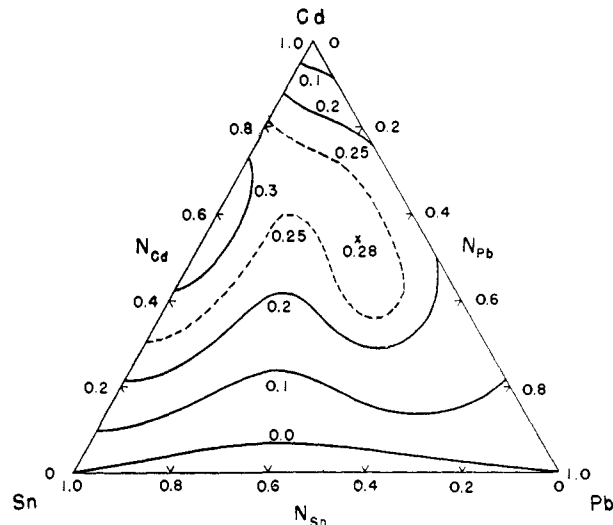


Fig. 25.—Excess molal entropy of solution surface ( $\Delta S^x$ ) for the cadmium-lead-tin solution at 500° in 0.1 calories/°C. steps.

### Discussion of Results

**Treatment of Data.**—Darken's<sup>2</sup> treatment of ternary systems has proved suitable for the three ternary systems studied. The values of  $G_{\text{binary } 1-3}^x$  for Equation (12) as predicted from the ternary data (Equation 14) agree very well with the observed values from the binary systems lead-bismuth and lead-tin. The fact that the agreement in the case of the lead-antimony system is less precise is to be ascribed to the greater departure from ideality in the ternary system, cadmium-lead-antimony. In the case of such an irregular solution a larger number of pseudo-binary systems would have to be investigated to obtain an accuracy comparable to that found in the other systems. Even in this case, the agreement may be considered fairly good since each predicted result is the small algebraic sum of several relatively large numbers. On the same grounds it may be pointed out that the good agreement for the other two systems is in a measure fortuitous.

**Excess Free Energy.**—The excess molal free energy surfaces (Figs. 5, 14 and 23) for the three ternary systems conform substantially to what one would expect from knowledge of the corresponding curves for the component binary systems. The excess partial molal free energy curves (Figs. 8, 17 and 26) are more sensitive indicators of the behavior of the solutions. They also grade rather smoothly from one side of the ternary field to the other, showing at the same time more subtle changes in a few cases than do the molal free energy surfaces. The uncertainty in the derived curves F, G, J and K is much greater than for the other eight curves in each figure.

**Heat of Solution.**—The molal heat of solution surfaces (Figs. 6, 15 and 24) show substantially the same forms as do the corresponding  $\Delta F^x$

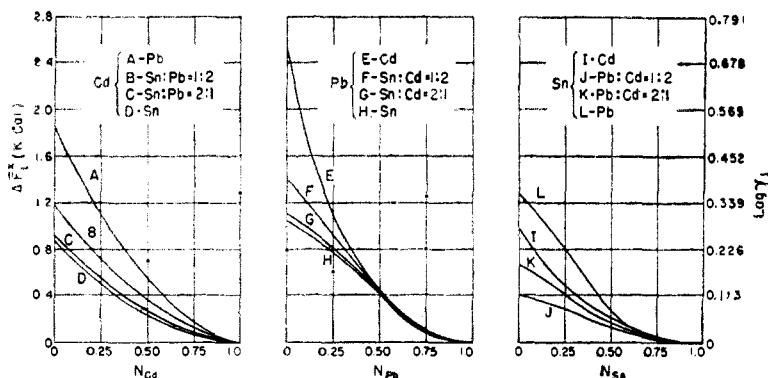


Fig. 26.—Excess partial molal free energy of solution curves in the cadmium-lead-tin solution at 500°.

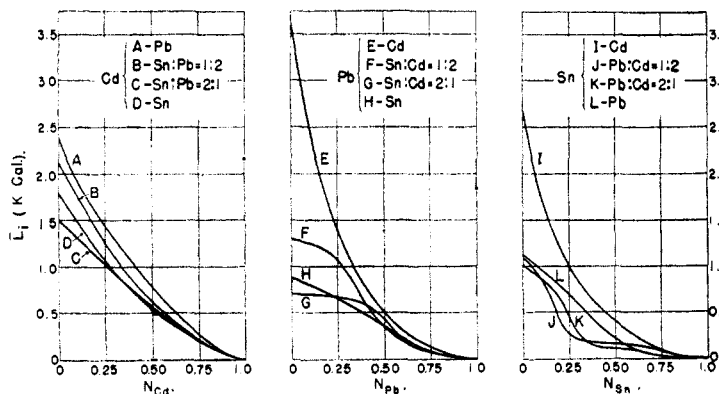


Fig. 27.—Relative partial molal heat of solution curves in the cadmium-lead-tin solution at 500°.

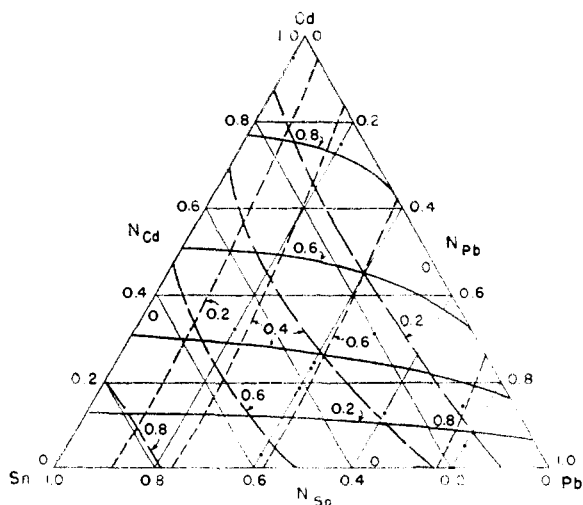


Fig. 28.—Isoactivity lines in the cadmium-lead-tin solution at 500°: activity lines: ———, cadmium; - - - - -, lead; - · - · -, tin.

surfaces. The cadmium-lead-tin solution is the only one showing the maximum  $\Delta H$  value as the crown of a "hill" well within the ternary field. The other two surfaces have their maxima on the cadmium-lead side and minima in the cadmium-antimony and lead-bismuth binaries.

**Excess Entropy.**—The excess molal entropy of solution surfaces are all positive for the three systems investigated except possibly in a very

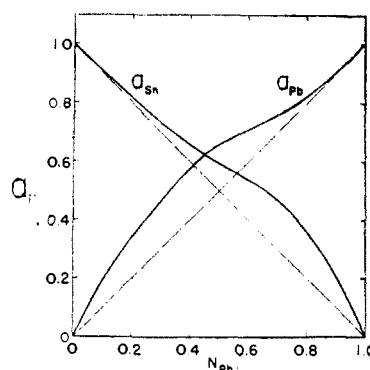


Fig. 29.—Activities in the lead-tin solution at 500°.

small portion of the cadmium-lead-tin solution. This is in accord with the positive excess entropies of solution for binary solutions which have been noted elsewhere.<sup>2,11,12</sup> The data leave some uncertainty in the position of the zero excess entropy contour in Fig. 25 and the small negative entropies recorded in Table VI may be considered equal to zero within the uncertainties of experiment and computation. There is no ready explanation for the entropy of solution being greater than ideal in the three solutions. Contributing in part probably is the positive excess volume of mixing

(11) J. Chipman and J. F. Elliott, "Symposium on Thermodynamics in Physical Metallurgy," Am. Soc. for Metals, Cleveland, Ohio, Oct., 1949, p. 102.

(12) O. J. Kleppa, *THIS JOURNAL*, **72**, 3346 (1950).

$(V - \sum_1^i N_i V_i^0)$  measured by Matuyama<sup>13</sup> for the liquid binary cadmium-lead, cadmium-bismuth and lead-bismuth systems and also for the equal-molar mixtures in the liquid ternary cadmium-lead-bismuth and cadmium-lead-tin solutions.

The three entropy surfaces illustrate the fallacy of seizing on relatively simple methods for predicting the thermodynamic behavior of liquid metallic solutions. For example, the virtually ideal entropy of mixing in the three binary systems, lead-bismuth, lead-antimony and lead-tin might lead one to guess

(13) Y. Matuyama, *Science Reports of the Tohoku Imperial University, Japan, Series 1*, **18**, 19 (1929).

that the three ternary cadmium systems should show strikingly similar entropy surfaces. Comparison of the three surfaces is sufficient to demonstrate the inadequacy of such an argument.

**Acknowledgments.**—The authors wish to express their appreciation to Donald L. Guernsey and Margaret Connors for analyses of the electrolytes and electrodes. They also wish to express their appreciation to the National Research Council for a predoctoral fellowship and to the Atomic Energy Commission for support of the investigation under Contract No. AT-30-GEN-368 (Scope I).

CAMBRIDGE, MASS.

RECEIVED DECEMBER 16, 1950

[CONTRIBUTION FROM THE MALLINCKRODT CHEMICAL LABORATORY, HARVARD UNIVERSITY]

## A New Multilayer Isotherm Equation with Reference to Surface Area

BY G. D. HALSEY, JR.

Using the London Law for the dispersion force causing multilayer adsorption and assuming various exponential distributions of sources for the force, coöperative multilayer isotherms are derived. Under certain circumstances these isotherms yield a surface area comparable to the BET area. Under other circumstances they reproduce, and explain deviations and pseudo-agreement with the BET treatment.

### Introduction

In an earlier paper<sup>1</sup> it was shown that on a uniform surface adsorption will take place coöperatively, at constant pressure, as soon as the coverage  $\theta$  reaches  $\sim 0.02$  of its saturation value. Furthermore, it was shown that in the absence of transmitted forces from the surface adsorption will proceed only to the depth of one layer, until the relative pressure  $p/p_0$  reaches unity, and bulk condensation begins. If an energy  $\Delta E_n$  in excess of the liquefaction energy is transmitted from the surface to the  $n$ 'th layer the  $n$ 'th layer condenses at a pressure

$$p/p_0 = \exp\{-\Delta E_n/RT\} \quad (1)$$

leading to an isotherm composed of a series of steps. If  $\Delta E_n$  falls off according to the usual inverse power law for dispersion forces, then  $\Delta E_n \sim 1/x^r$  where  $x$  is the distance from the surface. At large distances from the surface it would seem reasonable to replace  $x$  with  $\theta$ , since they are proportional, leading to the isotherm

$$p/p_0 = \exp\{a/RT\theta^r\} \quad (2)$$

The derivation implies that  $x$  varies continuously with  $\theta$ , while in actuality  $x$  can only be an integral multiple of the molecular diameter. Therefore (2) should be replaced by a step function, which is less than (2) except when  $\theta$  is integral. However, most real isotherms are smooth, and readily fitted by (2) as it stands, with  $r$  varying from  $\sim 1$  to  $\sim 10$ . Realizing that surface heterogeneity would tend to "smooth out" the step function, (2) was proposed as a semi-empirical isotherm.

However, as Hill has pointed out,<sup>2</sup> the value of  $r$  should be exactly three from the simple London treatment of dispersion forces, and somewhat larger if higher terms are included. The fact that for the

simple system nitrogen-anatase  $r = 2.67$ , lends some support to the approximate validity of (2). Nevertheless it is difficult to explain the small but definite deviation from  $r = 3$ , which is in the wrong direction and tends to get greater as  $\theta$  increases.

In what follows we shall show that the agreement achieved with (2) is accidental, and that the empirical value of  $r$  in (2) has no simple relation to the power in the expression for London forces.

In addition it should be pointed out that there is no reference to the volume of a monolayer in (2) and thus no indication of surface area. True enough, if  $r > \sim 2$ , the typical point of inflection and "point B" of the BET theory appears, but the position of this pseudo "point B" is clearly a function of temperature, and can have no reference to any particular degree of coverage in terms of monolayers. In the treatment of discrete layers which follows, this defect will be remedied.

### The Isotherm Equation

We have shown previously<sup>1</sup> that the isotherm equation for coöperative adsorption is merely the normalization integral of the distribution function of site-energies  $N(\Delta E)$  between the limits  $\Delta E = \infty$  and the  $\Delta E$  of eq. (1)

$$\theta_{(1)} = \int_{-RT \ln p/p_0}^{\infty} \frac{N(\Delta E) d\Delta E}{p/p_0} \quad (3)$$

The distribution function is normalized so that  $\theta_1 = 1$  when  $p/p_0$  reaches the condensation pressure of the bulk liquid adsorbate. We shall make the following assumptions: (1) The source of the van der Waals energy  $\Delta E$  has its origin one adsorbate diameter below the center of the first layer. (2)  $\Delta E$  decays with the third power of distance. (3) Regions of equal  $\Delta E$  are localized into large enough patches so that edge effects can be neglected.

Thus, in the second layer the distribution func-

(1) G. Halsey, *J. Chem. Phys.*, **16**, 931 (1948).

(2) *Ibid.*, **17**, 590 (1949).